Development of a New Particle Imaging Radiosonde with Particle Fall Velocity Measurements in Clouds

Kenji Suzuki[1], Yurika Hara[1], Takuji Sugidachi[2],
Kensaku Shimizu[2], and Masatomo Fujiwara[3]

[1]*Graduate School of Sciences and Technology for Innovation*, *Yamaguchi University*, *Yamaguchi*, *Japan*
[2]*Meisei Electric Co. Ltd.*, *Isesaki*, *Japan*
[3]*Graduate School of Environmental Science*, *Hokkaido University*, *Sapporo*, *Japan*

(Manuscript received 15 July 2023, accepted 14 September 2023)

Abstract A new particle imaging radiosonde "Rainscope" has been developed, and for the first time, particle fall velocity measurement functionality was added to a balloon-borne device. Rainscope can capture a clear still image of precipitation particles in a cloud when they interrupt an infrared beam, using a CMOS camera equipped with an electronic shutter. It can also record the time when a particle passes the upper and lower built-in infrared sensors, enabling measurement of the velocity of falling precipitation particles. For ground testing in rain and snow, a ground-based Rainscope showed raindrop/snowflake size-fall velocity distributions similar to those obtained in previous studies. In a comparison with a Parsivel2 disdrometer in rain, the Rainscope results were in good agreement with the distributions obtained by an adjacent Parsivel2. In a test flight of Rainscope into a stratiform cloud, raindrops, mostly melted particles, snowflakes in the process of melting, graupel, and snowflakes were observed. It was observed that the fall velocity varied depending on the type of solid precipitation particles.

Citation: Suzuki, K., Y. Hara, T. Sugidachi, K. Shimizu, and M. Fujiwara, 2023: Development of a new particle imaging radiosonde with particle fall velocity measurements in clouds. *SOLA*, **19**, 261−268, doi:10.2151/sola.2023-034.

1. Introduction

It is very important to accurately describe cloud microphysical features, such as particle size, phase, number density, and type, and the processes of how particles form, grow, and fall within clouds, for the understanding of precipitation mechanisms. In addition to the number density of particles, the mass density is essential for determining the vertical distribution of water in a cloud. While it is easy to make direct observations to determine the size of precipitation particles in clouds, it is difficult to determine their mass. This is because solid particles vary greatly in density depending on their formation process. For example, the density of graupel varies from 0.05 to 0.89 g cm^{-3} (Pruppacher and Klett 1996). It is difficult to directly measure the density of particles in a cloud, but if we can measure the size and fall velocity of those particles, then we can draw conclusions about the vertical distribution of density and mass. Balloon-borne observations are useful for measuring vertical profiles.

To obtain vertical hydrometeor profiles, videosondes were developed in the 1980s. These are balloon-borne instruments that image precipitation/cloud particles in clouds and transmit video signals to the ground in real time: CPVS (Cloud particle video sonde) by Murakami et al. (1989) and HYVIS (Hydrometeor videosonde) by Murakami and Matsuo (1990). Takahashi (1990) also developed another videosonde that uses the same transmitter/receiver system to capture precipitation particles and measure their electric charge.

There have been many other challenges in capturing precipitation particle images in clouds. Snow crystal sonde (Magono and Tazawa 1966) produced replicas of falling snow crystals on a film coated with replica fluid. It is detached with a parachute by a pneumatically controlled switch and collected on the ground. Milochevich and Heymsfield (1997) developed a replicator sonde equipped with a beacon for recovery. Boussaton et al. (2004) developed a sensor with a video camera that measures particle charges. Waugh et al. (2015) developed a balloon-borne instrument with Particle Size, Image, and Velocity (PASIV) probe, equipped with a high-resolution camera to measure not only particle images but also the fall velocity distribution of particles by a modified Parsivel disdrometer above the camera viewing chamber. Wolf et al. (2018) developed a sonde that, like HYVIS, captures cloud particles on film. However, these images are not transmitted in real time and must be recovered after the instrument lands. Real-time data transmission allows efficient observations to be made without the need to search for fallen sensors.

The videosonde developed by Takahashi (1990) has a built-in infrared sensor in front of a horizontally mounted camera and a strobe. When a particle interrupts the infrared sensor, the strobe is triggered and a CCD camera captures a still image of the particle. It can capture images of particles as they are in the air, without contact. The data are trans-

Corresponding author: Kenji Suzuki, Graduate School of Sciences and Technology for Innovation, Yamaguchi University, Yoshida, Yamaguchi 753-8515, Japan. E-mail: kenjis@yamaguchi-u.ac.jp.

mitted to the ground as an analog video signal with a carrier-wave frequency of 1680 MHz. Starting with videosonde observations on Ponape Island (Takahashi and Kuhara 1993), this system was deployed in field projects such as HEIFE (Heihe River Basin Field Experiment), TOGA-COARE (Tropical Ocean–Global Atmosphere Coupled Ocean–Atmosphere Response Experiment), and MCTEX (Maritime Continent Thunderstorm Experiment), as well as in different climatic regions such as the Southeast Asian monsoon areas, the rainy-season areas in southwestern Japan, and winter snowfall areas (Takahashi et al. 1995a, 1995b; Takahashi and Keenan 2004; Takahashi 2006; Takahashi 2010; Takahashi and Suzuki 2010).

In the 2000s, Suzuki et al. (2012) developed a smaller, lighter, and less expensive videosonde receiving system. It had a GPS slave system to control the 1680-MHz receiving antenna by calculating azimuth and elevation angles from the location obtained from the 400-MHz GPS radiosonde (RS-11G manufactured by Meisei Electric Co. Ltd) attached to the videosonde. Furthermore, the development of image analysis software has greatly improved observation convenience. This allows simultaneous launches from multiple locations and multiple videosonde launches into the same precipitation cloud (Suzuki et al. 2016). In addition, it is now possible to quantify and evaluate particle shapes using the circularity and aspect ratio (Suzuki et al. 2014, 2018). However, the conventional videosonde has the disadvantage of analog video transmission, which results in significant image degradation as the distance from the antenna increases.

To mitigate the image degradation caused by analog video transmission, we developed a new particle imaging radiosonde, which is named Rainscope, with digital image transmission in the 400-MHz band using image compression technology. The newly developed Rainscope can provide much clearer particle images than conventional videosondes. This allows particle surface conditions, such as melting, aggregation and riming, to be determined, as well as quantitative evaluation of the particle shape. It is expected to yield a great deal of cloud physics information, especially regarding solid precipitation particles in the upper layers of clouds. Rainscope also has a new function to measure the fall velocity of each precipitation particle in clouds. The PASIV developed by Waugh et al. (2015) provides particle counts, size distributions, and fall velocity distributions of particles, but the fall velocity of each individual particle is not measured. The development of Rainscope is a new attempt using a balloon-borne instrument which must be inexpensive, compact, and lightweight.

Various types of ground-based disdrometers have been used for fall velocity measurements. The Parsivel disdrometer (Löffler-Mang and Joss 2000) can measure the size of precipitation particles and estimate the fall velocity by detecting changes in light intensity caused by falling precipitation particles intercepting a laser sheet, although it cannot measure the particle shape. The 2D Video Disdrometer (2DVD; Kruger and Krajewski 2002) has two high-speed line-scan cameras to record the three-dimensional shape, size, and fall velocity of precipitation particles. While it is easy to estimate fall velocity on the ground, such as with Parsivel and 2DVD, it is difficult to measure the fall velocity of precipitation particles in clouds. While airborne optical instruments are useful for the measurement of particle size distributions in clouds, they cannot measure their fall velocities. Balloon-borne instruments are useful for measuring vertical profiles within clouds. Thus, measurement of the vertical profile of particle fall velocity in clouds, which is expected to provide new insights into cloud physics, has been needed.

This paper introduces precipitation particle fall velocity measurements using the newly developed Rainscope and reports the results of ground tests and test flights.

2. Description of Rainscope

Rainscope is a balloon-borne instrument to capture particle images and to measure their fall velocity. Rainscope has two infrared sensors and LED illumination at the front top and bottom of a CMOS camera (Fig. 1). The built-in Raspberry Pi connects to a PC or mobile phone via Wi-Fi or a wired LAN to set up observations and to start transmitting radio waves. When a particle passes the upper sensor, the camera with an electronic shutter speed of 1/100,000 s captures a still image and simultaneously records the time of passage.

The particle images are compressed in Rainscope, and an image is transmitted to the ground by a 400-MHz carrier wave. Conventional videosonde use analog NTSC video signal transmission with a 1680-MHz carrier wave, which is equivalent to an image sampling frame rate of 30 fps. The analog video transmission degrades image quality as the communication distance increases because the line quality deteriorates. Rainscope using a 400-MHz meteorological data band can transmit high-quality images with a size of 10 Kbytes under a limited transmission speed of 52.48 Kbps. The captured images are first stored in an SD card in Rainscope and then transmitted to the ground sequentially, one image every 2 s. If there are many particles to be captured, images are transmitted during ascent after exiting the clouds or during descent after the balloon is burst.

The particle fall velocity is calculated from the difference in passing time and the distance between the sensors, considering the ascending rate of Rainscope and the influence of the vertical wind inside the cloud. The particle passing time is recorded in 0.1-ms increments by a timer that resets every 2 s. Another infrared sensor is placed 28 mm below the upper infrared sensor. Passage times are recorded for up to 10 particles every 2 s. The data are transmitted to the

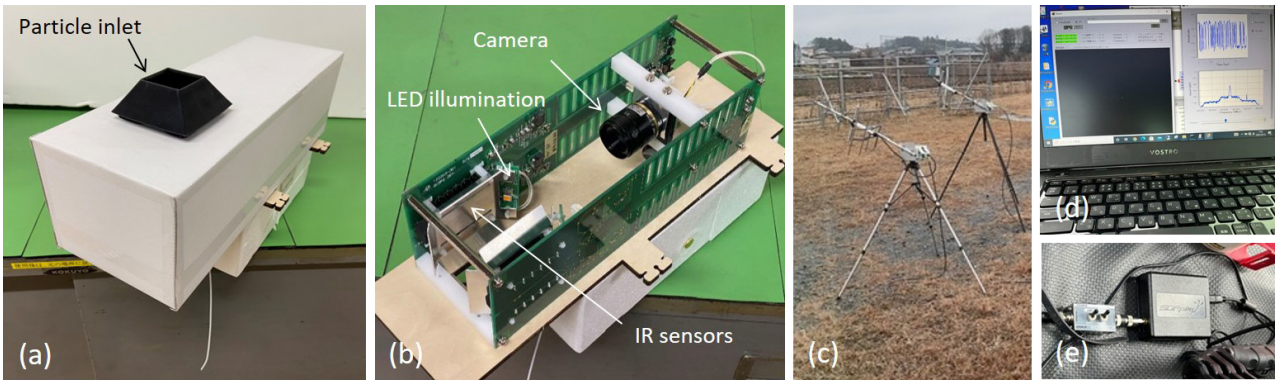

Fig. 1. (a) Exterior of Rainscope. (b) Interior of Rainscope, equipped with a camera, LEDs, and two infrared sensors. (c) 400-MHz band Yagi antenna for GPS radiosonde and Rainscope. (d) Image display on a PC. (e) Compact receiver.

Table 1. Specifications of Rainscope.

Particle sensor	Detection sensitivity	0.3 mm or larger (changeable)
	IR line sensor width	40 mm
	Illumination	White LED
Fall velocity sensor	Detector	2 IR line sensors
	Sensor distance	28 mm
Image	Field of view	32 × 24 mm
	Tone	Monochrome
	Resolution	640 × 480 Pixel
	Shooting interval	2 or 4 fps (selectable)
Transmitter	Carrier frequency	403.3–405.7 MHz (100 kHz interval)
	Occupied bandwidth	< 60 kHz
	Power	100 mW (20 dBm)
	Modulation method	FM-FSK
	Transmission speed	52.48 Kbps
	Transmission interval	0.5 fps
	Error correction	Reed-Solomon and Interleave
Operation time		180 min
Outlook	Size	354 (W) × 150 (D) × 199 (H) mm
	Weight	1100 g

ground and output as a CSV file. The ascending velocity data for an iMS100 GPS radiosonde (Meisei 2020) is used to calculate the fall velocity of particles. It is the moving average ascent rate over a 60-s period. This is because Rainscope attached to the balloon rises in a pendulum motion, and using an instantaneous value for the ascent rate would result in a large variation in the fall velocity.

Rainscope with iMS100 radiosonde provides the following data: particle image, temperature, humidity, wind speed, wind direction, altitude, particle size (long/short diameter, circumference, cross-sectional area), circularity, aspect ratio, and fall velocity of particles. Particle images are classified as raindrops, frozen drops (hail), graupel, ice crystals, or snowflakes on the basis of transparency (opaque or not), shape (smooth or irregular outline), and surface condition (melted or not). Rainscope is smaller and lighter than a conventional videosonde, and in consideration of the environment, the housing has been changed from metal to paper and wood. Specifications of Rainscope are shown in Table 1.

3. Results

3.1 Ground validation of fall velocity measurement of rain and snow

At Minamiuonuma (37.04°N, 138.85°E, 193 m above sea level), located in the mountainous area in the center of Japan's main island, Rainscope was installed on the ground and rain and snow measurement tests were conducted at the end of December 2021. Figure 2 shows particle images captured in the ground test of Rainscope. Rainfall was recorded from 0:07 to 1:08 JST on 22 December, with an hourly rainfall total of 1 mm. It was a weak rainfall with the observed raindrops having a diameter of up to 2 mm (Figs. 2a and 2b). A total of 1849 frames were imaged. The fall velocity could only be calculated if one particle was observed per frame because it was difficult to identify one particle falling past both infrared sensors. One raindrop per frame was observed in 931 frames, of which 738 (79% of the total) had

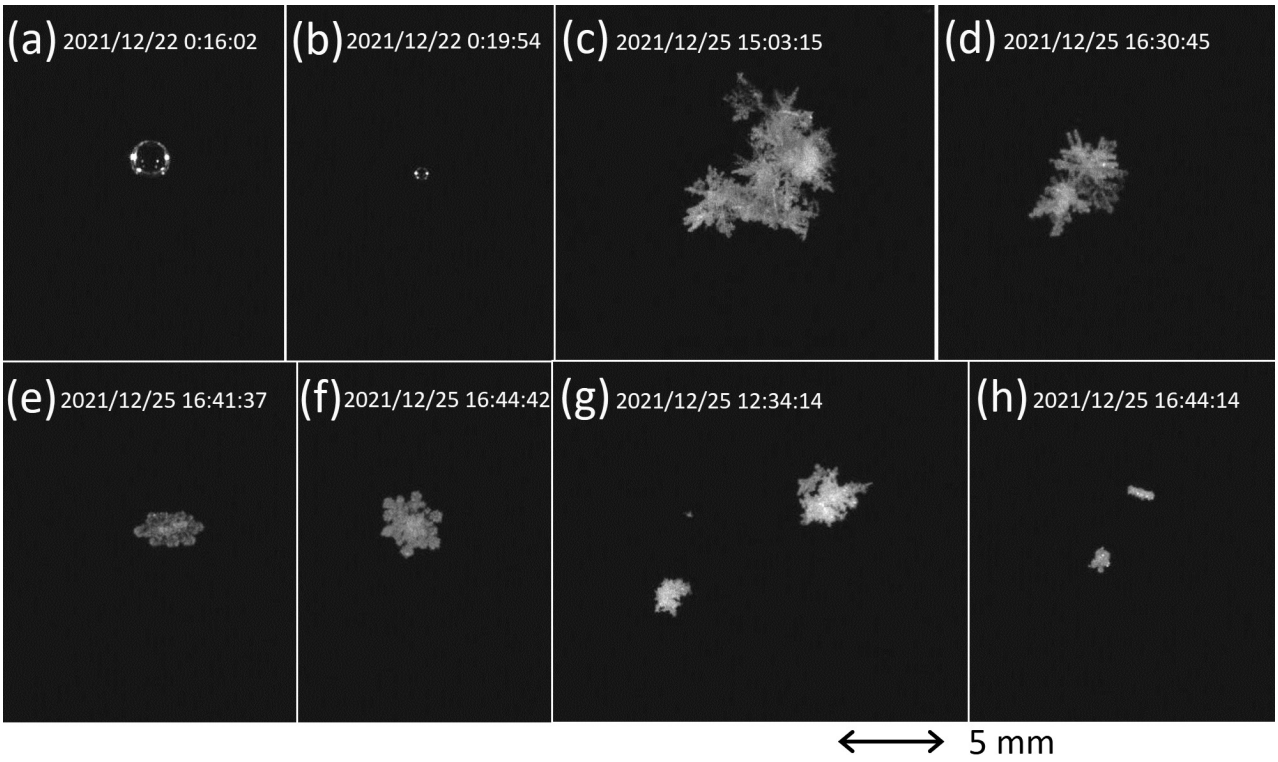

Fig. 2. Precipitation particle images obtained from Rainscope ground test at Minamiuonuma observation site on 22 and 25 December 2021.

fall velocities that could be calculated. When a particle falls diagonally, it may be detected by the upper sensor but not by the lower one, thus particle fall velocity cannot be calculated. Unfortunately, it is not possible to measure the falling velocity of all particles with the current specifications, because it is required reduction in size, weight, and cost for the disposable balloon-borne instrument.

In the observation on December 25, weak snow continued intermittently. Ground tests were performed from 12:12 to 15:19 and 16:29 to 16:52 JST, capturing 1745 frames; there were 829 frames with only one particle observed per frame, and the fall velocity was calculated for 710 particles (86% of the total). Snowflakes with aggregated needle and dendrite crystals (Figs. 2c and 2d) and a lot of ice particles of various shapes were observed (Figs. 2e–2h). No melting particles or heavy riming were observed.

Figure 3 shows the relationship between particle diameter and fall velocity in both the rain and snow cases. The results of the Rainscope ground test for raindrops were in good agreement with those of Atlas et al. (1973) except raindrops with a diameter of 1 mm or less tend to be underestimated. The fall velocity of snowflakes was less than 1 m s^{-1}, which is smaller than the rimed aggregate observed by Ishizaka (1995), but as shown in Figs. 2c and 2d, the observed snowflakes had almost no riming, and it can be assumed that their density was low, so the results can be considered to be reasonable. Particles with fall velocity close to zero are considered to be caused by particles that collide with the inlet and break up.

3.2 Comparison with ground-based disdrometer (Parsivel2)

A ground test was conducted on the Yamaguchi University campus (34.15°N, 131.47°E, 30 m above sea level) to compare the fall velocity measurement performance of Rainscope with that of Parsivel2 (visible laser model, firmware ver. 2.1.13), a widely used disdrometer. On 26 April 2022, the passage of a frontal line brought a steady rainfall of about 5 mm h^{-1}. Although each instrument could not measure the same raindrops, Rainscope was set up about 1 m away from Parsivel2 to observe the precipitation. Figure 4 shows the distribution of raindrop particle size and fall velocity observed from 11:00 to 11:10 JST on the same day. Both distributions of particle size and fall velocity were found to be generally consistent. There is a large difference in the number of observed raindrops, but this is thought to be due to the difference in sampling area and the shape of the particle intake. In conclusion, because the distribution of raindrop fall velocity measurements was similar to that of previous studies, such as Atlas et al. (1973) and Gunn and Kinzer (1949), and also similar to that of a general-purpose disdrometer, Rainscope's fall velocity measurements are considered to be reliable.

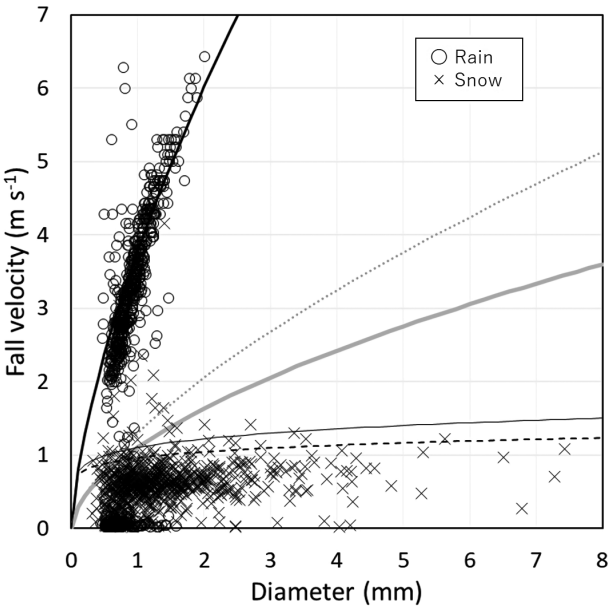

Fig. 3. Relationship between particle diameter and fall velocity in rain (circle) and snow (cross) during Rainscope ground tests in December 2021, with reference to Ishizaka et al. (2013). Black thick curve: Water droplet by Atlas et al. (1973), black thin curve: Densely rimed aggregates by Ishizaka (1995), black dashed curve: Rimed aggregates by Ishizaka (1995), gray dot curve: Lump graupel by Locatelli and Hobbs (1974), solid gray curve: Hexagonal graupel by Locatelli and Hobbs (1974).

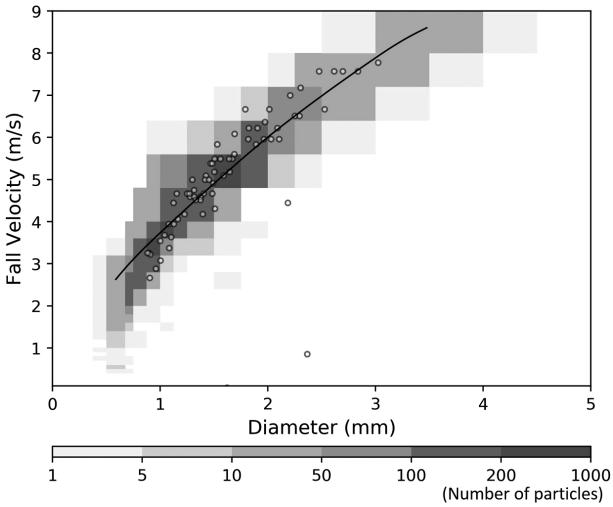

Fig. 4. Comparison of raindrop fall velocity observed by Rainscope and Parsivel2. A small circle shows a raindrop observed by ground-based Rainscope, and the gray scale shows the number of raindrops observed by Parsivel2 from 11:00 to 11:10 JST on 26 April 2022. Black curve indicates the empirical relationship curve of water droplet by Atlas et al. (1973).

3.3 Test flight of Rainscope into a stratiform cloud

From the Meisei Electric radiosonde test site at Mito (36.33°N, 140.42°E, 29 m above sea level), Rainscope was launched into a stratiform cloud associated with a developing low-pressure system on 20 February 2022, at 0:18 JST (Fig. 5a). A clear bright band was detected on radar. The AMeDAS in Mito recorded 4.5 mm of precipitation from 0:00 to 1:00 JST.

In addition to raindrops below the 0°C level, Rainscope observed various forms of solid precipitation particles near and above the freezing level, such as almost melted ice particles, partially melted snowflakes, hexagonal graupel and snowflakes (Fig. 5b). Previous videosonde observations could not capture such detailed particle surface conditions.

As shown in Fig. 6, the raindrop fall velocities had a distribution similar to those obtained by Atlas et al. (1973). Although not numerous, small snowflakes with a fall velocity of about 1 m s^{-1} were also observed. The fall velocity of the almost melted particles was distributed in the middle of the fall velocity of graupel and raindrops shown by the previous study. We thus confirmed that solid precipitation particles of different densities have different fall velocities. Differences in the fall velocity of solid particles indicate differences in particle density for the same particle size. This suggests the existence of different microphysical processes. The measurement of particle fall velocity in clouds will greatly contribute to the discussion of the graupel riming degree and the ice particle melting degree inside the melting layer.

However, in this test flight, the higher the altitude, the more difficult it was to calculate the particle fall velocity. This is because the particles that passed through the upper and lower infrared sensors cannot be identified when the particle number concentration becomes large. To address this problem, Rainscope has been improved. The minimum detection level of the infrared sensor can be increased, limiting the detection of smaller particles. In other words, we can focus on larger particles with larger fall velocity. In addition, to make it easier to identify particles that passed through the upper and lower sensors, a masking time of 10 ms was added to the infrared sensor after the first particle detection. As a result, we were able to calculate the fall velocity of 60% of the total particles in a ground test during snowfall (results not shown here). Our target is relatively large particles such as graupel and snowflakes in clouds. Measuring the fall velocity of individual particles with small diameter and large number concentration remains difficult.

4. Summary

A new precipitation particle imaging radiosonde (Rainscope) was developed to capture clear images and to measure the fall velocity of precipitation particles in clouds. Results of ground tests and test flights showed that raindrop fall ve-

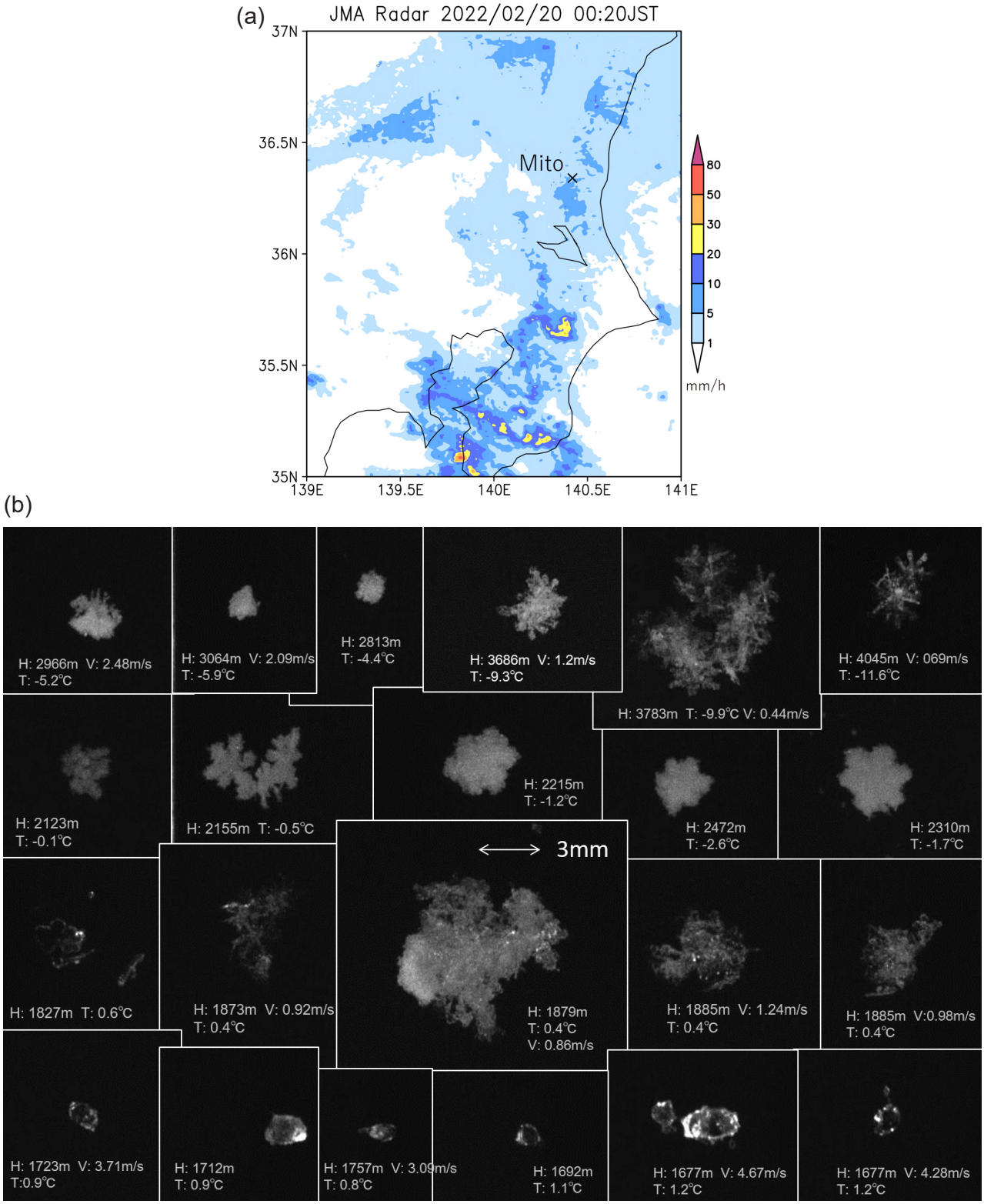

Fig. 5. (a) Japan Meteorological Agency radar image at 0:20 JST on 20 February 2022. (b) Particle images obtained from Rainscope test flight into stratiform cloud, launched from Mito observation site at 0:18 JST on 20 February 2022.

locities were close to the distributions obtained by Atlas et al. (1973) and to those measured by a Parsivel2 disdrometer. We also confirmed that the fall velocity of solid precipitation particles can be measured even in clouds. However, when the particle number concentration is large, the measurement of the fall velocity is difficult.

In addition to the detailed vertical profiles of precipitation particles obtained from clear images, the new information on particle fall velocity is expected to further our understanding of the cloud microphysics within clouds. We hope that Rainscope will bring new insights into the understanding of precipitation mechanisms.

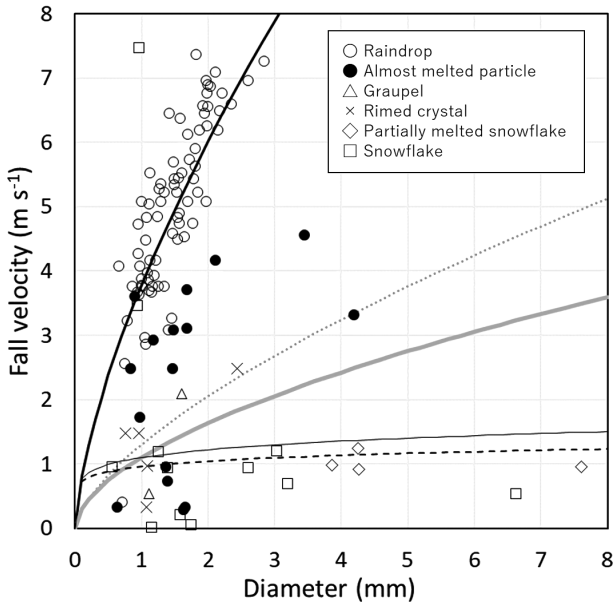

Fig. 6. Relationship between diameter and fall velocity of precipitation particles obtained from Rainscope test flight on 20 February 2022. Circle: raindrop, dot: almost melted particle, triangle: graupel, cross: rimed crystal, diamond: partially melted snowflake, square: snowflake. Empirical curves show the relationship between the particle size and the fall velocity on the ground as a reference, the same curves as in Fig. 3.

Acknowledgements

The present study was supported by the Strategic Information and Communications R&D Promotion Programme (SCOPE #195003007) of the Ministry of Internal Affairs and Communications (MIC) in Japan, and the Japan Aerospace Exploration Agency (JAXA) third research announcement on the Earth Observations research program under Grant JX-PSPC-539840.

Edited by: T. Ohigashi

References

Atlas, D., R. C. Srivastava, and R. S. Sekhon, 1973: Doppler radar characteristics of precipitation at vertical incidence. *Rev. Geophys.*, **11**, 1–35.

Boussaton, M. P., S. Coquillat, S. Chauzy, and F. Gangneron, 2004: A new videosonde with a particle charge measurement device for in situ observation of precipitation particles. *J. Atmos. Oceanic Technol.*, **21**, 1519–1531.

Gunn, R., and G. D. Kinzer, 1949: The terminal velocity of fall for water droplets in stagnant air. *J. Meteor.*, **6**, 243–248.

Ishizaka, M., 1995: Measurement of falling velocity of rimed snowflakes. *Seppyo*, **57**, 229–238 (in Japanese).

Ishizaka, M., H. Motoyoshi, S. Nakai, T. Shiina, T. Kumakura, and K. Muramoto, 2013: A new method for identifying the main type of solid hydrometeors contributing to snowfall from measured size-fall speed relationship. *J. Meteor. Soc. Japan*, **91**, 747–762.

Kruger, A., and W. F. Krajewski, 2002: Two-dimensional video disdrometer: A description. *J. Atmos. Oceanic Technol.*, **19**, 602–617.

Locatelli, J. D., and P. V. Hobbs, 1974: Fall speed and mass of solid precipitation particles. *J. Geophys. Res.*, **79**, 2185–2197.

Löffler-Mang, M., and J. Joss, 2000: An optical disdrometer for measuring size and velocity of hydrometeors. *J. Atmos. Ocean. Tech.*, **17**, 130–139.

Magono, C., and S. Tazawa, 1966: Design of a “snow crystal sonde”. *J. Atmos. Sci.*, **23**, 618–625.

Meisei Electric Co. Ltd., 2020: GPS Radiosonde iMS-100. (Available online at: https://www.meisei.co.jp/english/wp-content/uploads/2020/05/ims-100-e.pdf, accessed 30 April 2022)

Miloshevich, L. M., and A. J. Heymsfield, 1997: A balloon-borne continuous cloud particle replicator for measuring vertical profiles of cloud microphysical properties: Instrument design, performance, and collection efficiency analysis. *J. Atmos. Oceanic Technol.*, **14**, 753–768.

Murakami, M., T. Matsuo, T. Nakayama, and T. Tanaka, 1989: Development of cloud particle video sonde. *J. Meteor.*

Soc. Japan, **65**, 803–809.

Murakami, M., and T. Matsuo, 1990: Development of the hydrometeor videosonde. *J. Atmos. Oceanic Technol.*, **7**, 613–620.

Pruppacher, H. R., and J. D. Klett, 1996: *Microphysics of Clouds and Precipitation, Second Edition*. Kluwer Academic Publishers, 976 pp.

Suzuki, K., K. Shimizu, T. Ohigashi, K. Tsuboki, S. Kawamura, K. Nakagawa, K. Yamaguchi, and E. Nakakita, 2012: Development of a new videosonde observation system for in-situ precipitation particle measurement. *SOLA*, **8**, 1–4.

Suzuki, K., M. Matsuo, E. Nakano, S. Shigeto, K. Yamaguchi, and E. Nakakita, 2014: Graupel in the different developing stages of Baiu monsoon clouds observed by videosondes. *Atmos. Res.*, **142**, 100–110.

Suzuki, K., N. Munechika, K. Nakagawa, K. Yamaguchi, and E. Nakakita, 2016: Simultaneous measurements of a stratiform cloud by multipoint videosonde launchings. *SOLA*, **12**, 10–13.

Suzuki, K., K. Nakagawa, T. Kawano, S. Mori, M. Katsumata, F. Syamsudin, and K. Yoneyama, 2018: Videosonde-observed graupel in different rain systems during Pre-YMC project. *SOLA*, **14**, 148–152.

Takahashi, T., 1990: Near absence of lightning in tropical rainfall producing Micronesian thunderstorms. *Geophys. Res. Lett.*, **17**, 2381–2384.

Takahashi, T., 2006: Precipitation mechanisms in East Asian monsoon: Videosonde study. *J. Geophys. Res.*, **111**, D09202, doi:10.1029/2005 JD006268.

Takahashi, T., and K. Kuhara, 1993: Precipitation mechanisms of cumulonimbus clouds at Pohnpei, Micronesia. *J. Meteor. Soc. Japan*, **71**, 21–31.

Takahashi, T., and T. D. Keenan, 2004: Hydrometeor mass, number, and space charge distribution in a “Hector” squall line. *J. Geophys. Res.*, **109**, D16208, doi:10.1029/2004JD004667.

Takahashi, T., 2010: The videosonde system and its use in the study of East Asian monsoon rain. *Bull. Amer. Meteor. Soc.*, **91**, 1231–1246.

Takahashi, T., and K. Suzuki, 2010: Development of negative dipoles in a stratiform cloud layer in a Okinawa “Baiu” MCS system. *Atmos. Res.*, **98**, 317–326.

Takahashi, T., K. Suzuki, M. Orita, M. Tokuno, and R. de la Mar, 1995a: Videosonde observations of precipitation processes in equatorial cloud clusters. *J. Meteor. Soc. Japan*, **73**, 509–534.

Takahashi, T., K. Suzuki, C. Wang, and C. Guo, 1995b: Precipitation mechanisms of cloud systems developed in a semi-arid area of Pingliang, China: Videosonde observations. *J. Meteor. Soc. Japan*, **73**, 1191–1211.

Waugh, S. M., C. L. Ziegler, and D. R. MacGorman, 2015: In situ microphysical observations of the 29–30 May 2012 Kingfisher, OK, supercell with a balloon-borne video disdrometer. *J. Geophys. Res.*, **123**, 1–23.

Wolf, V., T. Kuhn, M. Milz, P. Voelger, M. Krämer, and C. Rolf, 2018: Arctic ice clouds over northern Sweden: Microphysical properties studied with the Balloon-borne Ice Cloud particle Imager B-ICI. *Atmos. Chem. Phys.*, **18**, 17371–17386.